

## **A Bidirectional Long Short Term Memory Approach for Infrastructure Health Monitoring Using On-board Vibration Response**

Authors:

Reza Riahi Samani  
Delft Center for Systems and Control  
Delft University of Technology  
E-mail: r.riahisamani@tudelft.nl

Alfredo Nunez Vicencio  
Section of Railway Engineering  
Delft University of Technology  
E-mail: a.a.nunezvicencio@tudelft.nl

Bart De Schutter  
Delft Center for Systems and Control  
Delft University of Technology  
E-mail: b.deschutter@tudelft.nl

**ABSTRACT**

The growing volume of available infrastructural monitoring data enables the development of powerful data-driven approaches to estimate infrastructure health conditions using direct measurements. This paper proposes a deep learning methodology to estimate infrastructure physical parameters, such as railway track stiffness, using drive-by vibration response signals. The proposed method employs a Long Short-term Memory (LSTM) feature extractor accounting for temporal dependencies in the feature extraction phase, and a bidirectional Long Short-term Memory (BiLSTM) networks to leverage bidirectional temporal dependencies in both the forward and backward paths of the drive-by vibration response in condition estimation phase. Additionally, a framing approach is employed to enhance the resolution of the monitoring task to the beam level by segmenting the vibration signal into frames equal to the distance between individual beams, centering the frames over the beam nodes. The proposed LSTM-BiLSTM model offers a versatile tool for various bridge and railway infrastructure conditions monitoring using direct drive-by vibration response measurements. The results demonstrate the potential of incorporating temporal analysis in the feature extraction phase and emphasize the pivotal role of bidirectional temporal information in infrastructure health condition estimation. The proposed methodology can accurately and automatically estimate railway track stiffness and identify local stiffness reductions in the presence of noise using drive-by measurements. An illustrative case study of vehicle-track interaction simulation is used to demonstrate the performance of the proposed model, achieving a maximum mean absolute percentage error of 1.7% and 0.7% in estimating railpad and ballast stiffness, respectively.

**Keywords:** Deep Learning, Infrastructure Health Monitoring, Vibration Response, Railway Track Stiffness

## 1 INTRODUCTION

Infrastructure health monitoring is a fundamental component of maintaining a safe and reliable infrastructure network. Continuous monitoring over time and across the infrastructure network facilitates the infrastructure health conditions estimation, which can be used for condition-based maintenance strategies (1, 2). This process involves assessing infrastructure damage, and tracking changes in physical properties, such as modal frequencies, modal mass, modal damping, stiffness, and mode shapes (3, 4).

In railway systems, monitoring the physical properties of infrastructure is crucial for capturing changes due to dynamic train loading and aging track components. Track stiffness forms a primary feature determining the degradation progress of railway infrastructure (5, 6). A sudden change in track stiffness is often related to changes in track type or associated to local damage to the ballast, substructure, and subgrade (fouled ballast, mud pumping, or hanging ties). Moreover, track stiffness is influenced by the superstructure and missing/graded fastening components (7). Given the determining nature of track stiffness for railway condition estimation, accurate measurements of this property can significantly support maintenance decisions.

Infrastructure health conditions can be measured indirectly under both loaded and unloaded conditions using dynamic loads or external excitation forces. Two common techniques for measuring health conditions under loaded conditions are pass-by and vehicle-based (drive-by) measurements (8). Pass-by measurements are typically used for specific locations of interest and involve placing a network of accelerometers to record vibration responses at strategic points, such as bridges. These methods incur costs for sensor deployment and limit measurements to a single location. Consequently, vehicle-based measurements have become increasingly preferred since they present high-accuracy and cost-effective measurements along the entire infrastructure network.

Traditionally, infrastructure physical parameter estimation methods relied on sophisticated identification algorithms to solve inverse problems in modal parameter estimation (9–11). For example, (10, 11) investigated track stiffness estimation using optimization techniques namely, cross-entropy (10) and adaptive regularization (11) to solve the identification optimization problem and to infer the railway track stiffness profile. However, implementing such algorithms is often computationally expensive and time-consuming (12). Furthermore, the centralized nature of parametric damage detection methods makes them infeasible for real-time damage detection applications, especially as infrastructure data continues to grow exponentially. Hence, recent advances in machine learning, particularly deep learning techniques, offer promising alternatives for overcoming these challenges (13–16).

In the current paper, we further explore the estimation of infrastructure physical parameters through deep learning approaches. We consider railway infrastructure to demonstrate the application of our proposed methodology in estimating railway track stiffness parameters using vibration response signals. Railway inspection often relies on Axle Box Acceleration (ABA) monitoring systems (7, 17, 18), hence, we utilize ABA measurements to estimate track stiffness. Furthermore, our methodology holds promise for broader applications in infrastructure inspections utilizing drive-by vibration measurements. For further information on drive-by infrastructure inspections, readers can refer to (19).

### 1.1 Deep learning in structure health monitoring using vibration response

Deep learning techniques have increasingly gained attention in infrastructure health monitoring in recent years. The strength of these techniques to detect and locate damage directly from vibration response without any need for data preprocessing or hand-crafted feature extraction is highly promising compared to traditional vibration-based structure monitoring techniques (12). Deep learning techniques generally require a two-stage process including a damage-sensitive feature extraction through the raw acceleration signals, and processing the extracted features to assess the health state of the structure (12, 20). Accordingly, an

autoencoder-based framework has been proposed by (20) for structural damage identification, comprising two main components: dimensionality reduction and relationship learning. The first component reduces the dimensionality of the original input vector, and the second component learns the relationship between the features and the stiffness reduction. Furthermore, (21) proposed a convolutional neural network (CNN) framework to predict the track dynamic stiffness using the ABA measurements in real-time, including a comparison of the performance between the standard CNN and dilated CNN algorithms. Both models performed well considering their accuracy, with the dilated CNN requiring less computation time in both the training and deployment processes. While CNN effectively captures relevant information within a neighborhood of samples, it often struggles to learn long-term dependencies in sequential datasets, which is relevant for railway track parameter estimation over a long period of data. To address this, (22) proposed a 1DCNN-LSTM-ResNet architecture to identify structural damages based on time-dependent data. The model employs one-dimensional CNN (1DCNN) for feature extraction, Long Short-term Memory (LSTM) for recognizing long-term dependencies, and ResNet to counteract the vanishing gradient problem during deep network training. The proposed architecture outperformed 1DCNN, LSTM, and their combination in diagnosing the damage states of the Z24 bridge located in the Bern district near Solothurn, Switzerland.

Moreover, structure health monitoring has been addressed with anomaly detection approaches. The papers (23), (24) developed LSTM-based anomaly detection frameworks to identify vibration sequence anomalies in subway tracks and bridges, respectively. The LSTM model was trained only on normal sequences, and the anomaly score was estimated via the reconstruction error between the model input sequence and output sequence. The input sequence was identified as an anomaly sequence through comparison to the anomaly threshold value. Although the anomaly detection approach is highly applicable when there are limited available data of malfunction conditions, since the model's training process is biased towards normal cases, it may not generalize well to abnormal situations.

## 1.2 Contributions of the paper

In this paper, we propose an innovative model architecture, namely, LSTM-BiLSTM networks, to estimate infrastructure physical parameters using vehicle-based vibration responses. This work makes the following contributions with respect to the state-of-the-art. First, our work highlights the pivotal role of the bidirectional temporal dependencies in both the forward and backward paths of the vibration response of the infrastructure. The idea stems from the fact each sequence of vibration responses is influenced by both the forward and backward paths of the infrastructure's vibration response. By using BiLSTM networks, we can effectively capture and integrate these temporal relations, leading to more accurate infrastructural health condition estimations. Second, we enhance the infrastructure monitoring resolution to beam nodes using the proposed framing approach to leverage accurate vibration signal positions. This framing approach segmentizes the vibration response within bearing spans over the beam nodes, which facilitates localized condition estimation at individual beam resolutions. Thirdly, the methodology employs a novel feature extraction method based on an LSTM layer and proposes the potential of incorporating temporal relations even at the feature extraction level. Our model exhibits excellent performance in a case study focusing on railway track segments, demonstrating accurate estimation of railpad and ballast stiffness, and identifying local stiffness reductions in a noisy environment.

## 2 PRELIMINARIES

### 2.1 LSTM cell

LSTM was introduced as an enhancement over traditional Recurrent Neural Networks (RNNs) for long-term dependency (25). The LSTM network captures temporal dependencies with additional memory cells. An

LSTM memory cell controls the flow of information and handles the memory efficiently using three types of gates: input, forget, and output gate as shown in Figure 1. Given a time series input  $x = (x_1, \dots, x_T)$ , where  $T$  represents the last time step  $t$ , LSTM updates the hidden state  $h_t$  using current input information  $x_t$ , hidden prior information state  $h_{t-1}$ , input gate  $g_{i,t}$ , forget gate  $g_{f,t}$ , output gate  $g_{o,t}$  and a memory cell  $c_t$ . The mathematical expression for a forward pass of an LSTM unit can be defined as

$$g_{i,t} = \sigma(W_{xi}x_t + W_{hi}h_{t-1} + b_i) \quad (1)$$

$$g_{f,t} = \sigma(W_{xf}x_t + W_{hf}h_{t-1} + b_f) \quad (2)$$

$$g_{o,t} = \sigma(W_{xo}x_t + W_{ho}h_{t-1} + b_o) \quad (3)$$

$$\tilde{c}_t = \tanh(W_{x\tilde{c}}x_t + W_{h\tilde{c}}h_{t-1} + b_{\tilde{c}}) \quad (4)$$

$$c_t = g_{i,t} \otimes \tilde{c}_t + g_{f,t} \otimes c_{t-1} \quad (5)$$

$$h_t = g_{o,t} \otimes \tanh(c_t) \quad (6)$$

$$y_t = \sigma(W_yh_t + b_y) \quad (7)$$

where the notations  $\otimes$  is an operator for point-wise multiplication of vectors,  $\varphi$ , and  $\sigma$  are the  $\tanh$  and sigmoid activation functions respectively, and  $W$  and  $b$  are respectively weight matrices and bias parameters for each LSTM cell. Moreover,  $\tilde{c}_t$  denotes the cell input activation vector, and  $c_t$  and  $c_{t-1}$  denotes the cell state values at time steps  $t$  and  $t-1$  respectively. The input gate  $g_{i,t}$  determines the cell state that needs to be updated, the forget gate  $g_{f,t}$  decides what information should be overlooked, and the output gate  $g_{o,t}$  determines which part of the cell state should be exported.

A cell state  $c_t$  consists of two components: i)  $g_{i,t} \otimes \tilde{c}_t$ , which includes the relevant information from  $\tilde{c}_t$  through  $g_{i,t}$  and ii)  $g_{f,t} \otimes c_{t-1}$ , which forgets the less-relevant information from  $c_{t-1}$ . In the final step, the hidden state  $h_t$  is employed to predict  $y_t$  at each time step. The entire network is parameterized with the weight matrices and bias parameters and is learned during backpropagation.

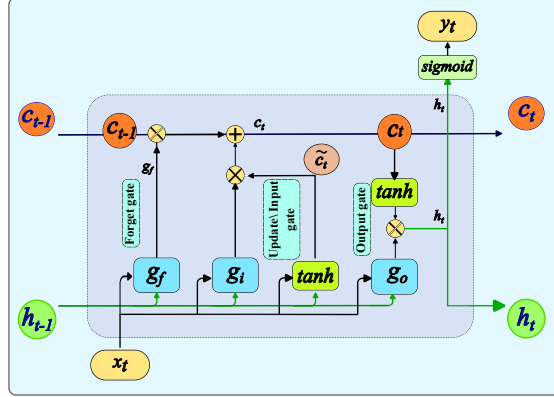


**FIGURE 1** Long Short Term Memory (LSTM) cell. The fundamental components of an LSTM cell are a forget, input, and output gate, updating cell state, and hidden state.

## 2.2 1D Convolutional Neural Networks

One-dimension Convolutional Neural Networks (1DCNNs) are recognized in deep learning for their proficiency in handling local relationships in sequential and time-series data. A basic 1DCNNs comprises several

1D filters in the 1DCNN layer and 1D pooling layers to capture the spatial patterns by applying the convolution operation. During this process, filters slide across time steps, creating feature maps that capture detailed and abstract representations of the data's patterns. Feature maps are essentially the outputs of the convolution process, depicting different aspects of the input data. Moreover, pooling layers complement this by downsampling the outcome of the convolution process, effectively emphasizing important features while reducing computational load. Max pooling or average pooling layers are commonly used to summarize the feature maps by reducing their spatial dimensions and highlighting salient features in the process.

The formula of one typical convolutional layer is:

$$h_f = \text{conv1D}(W_f, x) + b_f \quad (8)$$

where  $h_f$ ,  $W_f$  and  $b_f$  are respectively the output vector, weight matrices, and bias parameter of the filter  $f$ , while  $x$  is the input vector and  $\text{conv1D}$  is the 1D convolution operator whose  $i^{th}$  output is calculated by the following formula:

$$\text{conv1D}(W_f, x(i)) = W_f \otimes x(i) = \sum_{j=1}^{N_f} w_{fj} x_{i-j} \quad (9)$$

where  $N_f$  is the length of the filter  $f$ , and  $w_{fj}$  is the  $j^{th}$  element of matrices  $W_f$ .

### 3 METHODOLOGY

#### 3.1 Problem statement

Infrastructure health condition estimating using vehicle-based vibration response requires spatial and temporal analysis of the vibration signals. We approach the drive-by vibration response as a sequence of vibration signals associated with the sequence of beams and their physical properties. Our framing approach segmentises the vibration response signal with the spans, equal to the distances between individual beams, and located at the beam nodes. These bearing spans are associated with the lengths where, under normal conditions, a beam node bears a relative load between the beam nodes. By segmenting the vibration signal over the bearing spans at the beam nodes, we leverage domain knowledge about the position of beams and the vibration signal, enhancing the resolution of infrastructure health monitoring at the beam level. For instance, in the case of railway track monitoring, the vibration signal is framed for each sleeper as a beam node, with the length of the bearing span equal to the distance between individual sleepers, centred at each sleeper position. Consequently, the sequential model can estimate health conditions in a sequential manner at the resolution of individual sleepers.

The proposed approach involves a multi-level sequential data analysis. First, the lower-level network performs the feature extraction task over the vibration response segments. Second, the upper-level BiLSTM network takes the extracted features to estimate the health conditions over the sequence of beams. In the following, Section 3.2 discusses the lower-level bearing span feature extraction methods, followed by Section 3.3, which discusses the upper-level BiLSTM networks for the estimation of health conditions.

#### 3.2 Lower level bearing span feature extractor

##### 3.2.1 1DCNN

The idea behind using 1DCNN in the feature extraction phase is to leverage the strength of 1DCNN in capturing local relationships in this phase. The 1DCNN can provide features for the upper-level model based

on local relations within the input signal. The 1DCNN architecture used in this paper comprises three sets of convolutional and max-pooling layers, followed by a flattening layer and a fully connected layer that constructs the output layer of the feature extraction. The hyperparameters of the network include the number of convolutional layers, the number of filters in each layer, filter lengths, and the size of the dense layer, which is the latent space size of the feature extractor. Features extracted from the network are fed as the input for the subsequent model in the upper-level analysis.

While 1DCNNs emphasise the local patterns in the input sequence, they can be less efficient in capturing temporal dependencies, especially when the filter size is not sufficiently large. However, Recurrent architectures, such as LSTMs, effectively address this challenge by capturing temporal information using their cell memory. Hence, we also investigate the performance of an LSTM feature extractor in the feature extraction phase.

### 3.2.2 LSTM Cell

In contrast to the previous approach, this feature extractor aims to emphasise the temporal relationships within the input sequence. While the vibration signal exhibits long-term temporal relations in the upper-level beam-to-beam context, the LSTM-based feature extractor can also be incorporated to emphasise temporal relations within the feature extraction phase. The feature extractor used in this paper consists of an LSTM layer that takes the frames of vibration signals and returns the hidden state of the last time step as the extracted features for each frame. The extracted features are fed as the input for the subsequent BiLSTM networks in the upper-level analysis. The hyperparameters of the feature extractor include the number of LSTM layers and the number of LSTM units per layer.

## 3.3 Upper-level BiLSTM Networks

After extracting features from the bearing span frames in the lower-level analysis, the output is fed into BiLSTM networks at the upper level to capture the long-term temporal relations between sequences of beams. This approach is based on the physics of vehicle-based vibration response signals, where sequences are related to both the forward and backward paths of the sequence. For example, when there is a defect in one of the beams in a sequence, it is reflected not only in the forward path of the drive-by vibration signal but also in the backward path. Therefore, we propose using BiLSTM networks, which consist of stacking two BiLSTM layers, and the outputs of the layers are concatenated and passed to the subsequent layers. The bidirectional information is fed to the final fully connected networks to produce the output vector. The hyperparameters include the number of BiLSTM layers, the units of each layer, and the units of the fully connected networks. The schematic view of the BiLSTM networks is provided in Figure 2.

## 4 ILLUSTRATIVE CASE STUDY OF RAILWAY TRACK MONITORING

Railway track stiffness is a key indicator of the track's health and is commonly used to monitor the condition of the infrastructure. This stiffness is primarily influenced by the stiffness of the ballast, but it is also affected by the stiffness of the fastening systems, which include bolts, clamps, and rail pads. In this paper, track stiffness is considered by railpad and ballast stiffness parameters, denoted as the vector  $k = [k_p, k_b]^\top$ , where the influence of fastening components is considered via railpad stiffness. The objective of the analysis is to estimate the track stiffness using observed Axle-Box Acceleration (ABA) vibration responses.

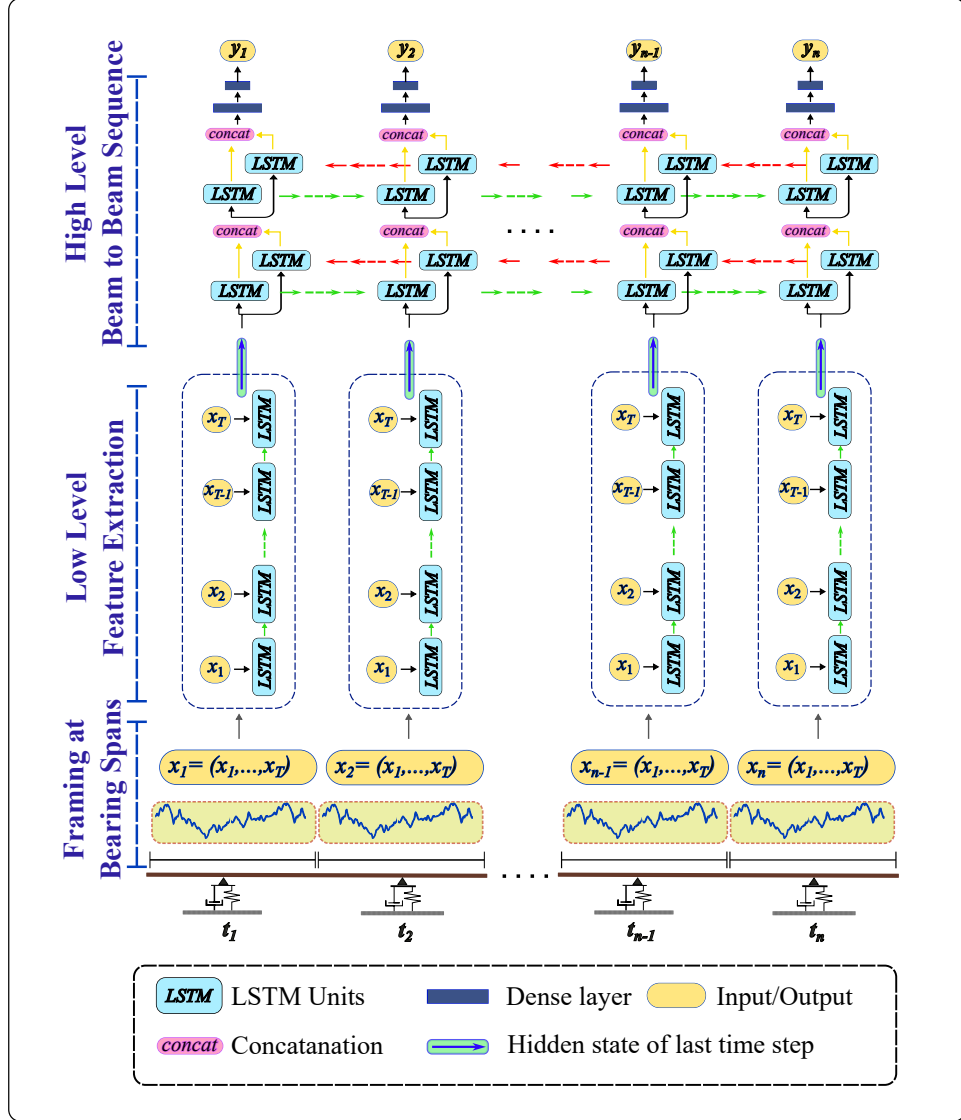


**FIGURE 2** Model architecture of the proposed LSTM-BiLSTM model.

#### 4.1 Data

Data preparation for this case study is conducted using the finite element model proposed in (7). This model accurately represents the physics of the vehicle-track interaction and simulates ABA measurements at an operational speed of 65 km/h by solving the vehicle-track motion equation. The dataset includes cases of constant track stiffness and local changes in track stiffness related to the railpad and ballast stiffness. Constant track stiffness represents the normal condition of railway tracks, where there is no change in track stiffness along the track. Ballast and railpad stiffness values in the simulation model are randomly selected from the stiffness range set R1 in Table 1, using a uniform distribution.

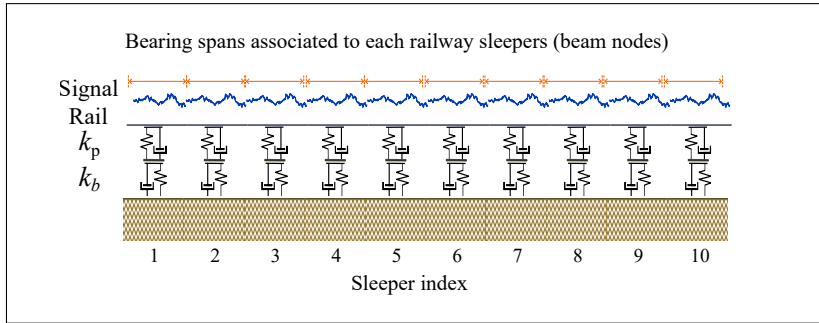
The stiffness reduction is considered in two scenarios: reduction in one sleeper and reduction in three sleepers within a 10-sleeper segment at random locations. The stiffness reduction in one sleeper simulates a defect such as a hanging sleeper, where an unsupported sleeper hangs within the railway segment, causing a local reduction in track stiffness at that sleeper. The stiffness reduction in three sleepers simulates a scenario where a reduction in substructure support over a wider length leads to reduced stiffness in multiple

**TABLE 1 Range of parameter values used for railpad and ballast stiffness.**

Range sets (range of values of the model's parameters)	$k_p$ (N/M)	$k_b$ (N/M)
R1	$1.5 \cdot 10^8 - 3 \cdot 10^8$	$1.6 \cdot 10^7 - 2.2 \cdot 10^7$
R2	$0.1 \cdot 10^8 - 1.5 \cdot 10^8$	$0.4 \cdot 10^7 - 1.6 \cdot 10^7$

sleepers (7). The stiffness of the railpad and ballast are simultaneously reduced to the stiffness range set R2 in Table 1, using a random variable with uniform distribution. The stiffness range set R2 represents multiple faults with varying severities, including degraded or missing railpads or local reductions in ballast stiffness, indicating potential component degradation (7). The random locations of stiffness reduction within the track segment prevent biases in the spatial distribution of defects, making the simulations more representative of real-world scenarios.

To test the robustness of the proposed method in a noisy environment, which is relevant to drive-by vibration response observations, an additive white Gaussian noise  $\sim N(0, \sigma^2)$  is considered for the ABA signal, where  $\sigma$  is the standard deviation of the measurement noise. A noise-to-signal ratio of 15% is used, with a variance equal to 15% of the ABA signal power. The additive 15% Gaussian noise in the ABA signal is considered to simulate real-world conditions and evaluate the performance of the proposed model under such circumstances. Each of the noise-free and noise-added scenarios consists of 15 000 records of 10-sleeper track segments, and the datasets are split into training, validation, and test sets, with 60%, 20%, and 20% of the total records, respectively. Figure 3 illustrates the schematic view of a 10 sleeper track segment and the corresponding framing for the vibration response signal.

**FIGURE 3 The layout of the 10 sleepers track segment.**

## 4.2 Results

In this section, we present the performance of the proposed LSTM-BiLSTM networks in estimating track stiffness using railway ABA measurements. For comparison, we also consider three other model architectures: 1DCNN-LSTM, LSTM-LSTM, and 1DCNN-BiLSTM.

During the training and validation process, the data is split into training and validation sets. Figure 4 shows the training process of the four models (CNN-LSTM, LSTM-LSTM, CNN-BiLSTM, and LSTM-BiLSTM) on the noise-added datasets, demonstrating the loss convergence versus the number of epochs on a logarithmic scale. The figure indicates that the LSTM-BiLSTM architecture achieves the lowest training loss compared to the other models. The validation set is used to fine-tune the hyperparameters of the models using a grid search method. The performance of the selected fine-tuned models is then evaluated on the test set, with the results presented in Table 2. Two evaluation metrics, Mean Absolute Percentage Error

(MAPE) and Root Mean Square Error (RMSE), are used to compare the accuracy of the models in stiffness estimation. MAPE measures the average absolute percentage difference between predicted and actual values, while RMSE measures the square root of the average squared differences between predicted and actual values.

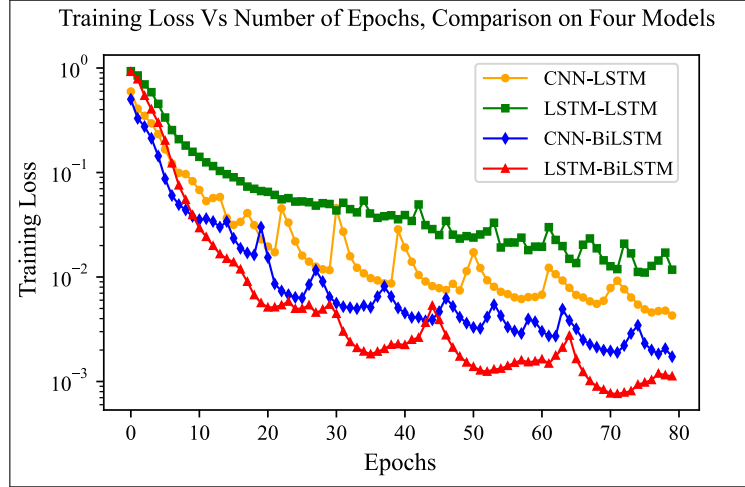


**FIGURE 4 Training loss convergence in the scenario of the noisy dataset.**

Table 2 shows the estimation accuracy performance of the four models (CNN-LSTM, LSTM-LSTM, CNN-BiLSTM, and LSTM-BiLSTM) on the test set under two conditions: noise-free and noise-added datasets. The performance metrics include Root Mean Squared Error (RMSE) and Mean Absolute Percentage Error (MAPE) for two parameters, railpad ( $k_p$ ) and ballast ( $k_b$ ) stiffness, along with an overall MAPE.

In a noise-free environment, the LSTM-BiLSTM model outperforms the other models, achieving the lowest RMSE for  $k_p$  at 0.82 (MN/m) and for  $k_b$  at 0.06 (MN/m). The MAPE values for LSTM-BiLSTM are also the lowest, with 0.61% for  $k_p$  and 0.35% for  $k_b$ , resulting in an overall MAPE of 0.47%. The CNN-BiLSTM model demonstrated the second-best performance in the noise-free condition. It recorded an RMSE of 2.81 (MN/m) for  $k_p$  and 0.14 (MN/m) for  $k_b$ . Its MAPE values are 1.76% for  $k_p$  and 0.74% for  $k_b$ , leading to an overall MAPE of 1.25%. The CNN-LSTM and LSTM-LSTM models rank below their BiLSTM counterparts, with overall MAPE of 1.66% and 1.92% respectively.

Under the 15% noise condition, the RMSE and MAPE values for all models increase. However, the LSTM-BiLSTM model remains the best performer, with an RMSE of 2.72 (MN/m) for  $k_p$  and 0.13 (MN/m) for  $k_b$ . The MAPE values are 1.70% for  $k_p$  and 0.70% for  $k_b$ , resulting in an overall MAPE of 1.20%. The CNN-BiLSTM model continued to show the second performance with an RMSE of 6.39 (MN/m) for  $k_p$  and 0.38 (MN/m) for  $k_b$ . The MAPE values were 3.90% for  $k_p$  and 1.57% for  $k_b$ , leading to an overall MAPE of 2.77%.

The LSTM-BiLSTM and CNN-BiLSTM models consistently outperform the other two models across both datasets. The LSTM-BiLSTM model, in particular, shows low RMSE and MAPE values, highlighting its superior capability in handling both noise-free and noisy data conditions. The LSTM-LSTM and CNN-LSTM models show almost similar performance in noise-free conditions; however, the LSTM-LSTM shows poorer performance under noise-added conditions. Overall, all models perform better in predicting ballast stiffness than railpad stiffness.

Figure 5 illustrates the ground truth and predictions for railpad and ballast stiffness in noise-free and noise-added conditions for six railway track segments. The ground truth values of stiffness parameters are represented by the black line, and the estimations in noise-free and noisy conditions are presented in

**TABLE 2** Models estimation accuracy performance on the test set in noise-free and (15%) noisy datasets.

Models	Noise-Free Dataset					Noisy Dataset				
	$k_p$		$k_b$		Overall	$k_p$		$k_b$		Overall
	RMSE	MAPE	RMSE	MAPE	MAPE	RMSE	MAPE	RMSE	MAPE	MAPE
<b>CNN-LSTM</b>	3.68	2.29%	0.18	1.04%	<b>1.66%</b>	8.59	5.15%	0.45	2.20%	<b>3.60%</b>
<b>LSTM-LSTM</b>	4.36	2.71%	0.25	1.12%	<b>1.92%</b>	11.71	6.41%	0.51	2.59%	<b>4.50%</b>
<b>CNN-BiLSTM</b>	2.81	1.76%	0.14	0.74%	<b>1.25%</b>	6.39	3.90%	0.38	1.57%	<b>2.77%</b>
<b>LSTM-BiLSTM</b>	0.82	0.61%	0.06	0.35%	<b>0.47%</b>	2.72	1.70%	0.13	0.70%	<b>1.20%</b>

blue and red lines, respectively. Railpad and ballast stiffness are estimated simultaneously in scenarios of constant track stiffness and local stiffness reduction in one and three sleepers.

### 4.3 Discussion

The illustrative case study demonstrated that the proposed LSTM-BiLSTM model effectively estimates infrastructure stiffness using vehicle-based vibration signals, achieving a MAPE of 1.70% for railpad stiffness and 0.70% for ballast stiffness in the noise-added scenario. The BiLSTM networks outperformed their LSTM counterparts, highlighting the importance of incorporating bidirectional information to enhance infrastructure health monitoring algorithms. The analysis shows that employing BiLSTM in the higher-level health condition estimation phase can reduce MAPE and RMSE by almost 50%, even in the presence of noise in the input signal. Hence, this model architecture holds promise for future research and practical applications, given the prevalence of various types of noise in drive-by vibration response measurements.

In the feature extraction phase, the results indicate a nuanced performance pattern among the four model architectures. The best-performing model, LSTM-BiLSTM, employs an LSTM layer in the feature extraction phase, demonstrating the potential of utilizing LSTM layers in this phase. This model outperforms the CNN-BiLSTM model, suggesting that LSTM's strength in capturing temporal dependencies can be more effective than CNNs when paired with BiLSTM networks. Moreover, the findings underscore the compatibility of BiLSTM networks with both CNN and LSTM feature extractors, as both CNN-BiLSTM and LSTM-BiLSTM models notably outperform their LSTM counterparts in noise-added scenarios.

The comparative performance of LSTM-LSTM and CNN-LSTM models introduces complexity in the evaluation of feature extraction methods. The LSTM-LSTM performance slightly falls behind the CNN-LSTM model, specifically in noise-added cases. This necessitates further investigation into the utilization of LSTM networks in the feature extraction phase. The literature supports the significance of frequency domain analysis in feature extraction phases, as highlighted in studies such as (7, 26, 27). Both approaches, LSTM layers, and time-frequency transformations, focus on capturing temporal dependencies along the signal. LSTM networks achieve this through memory cells that learn patterns over time, making them promising candidates for feature extraction (28, 29). This similarity points to an area for future research, where further

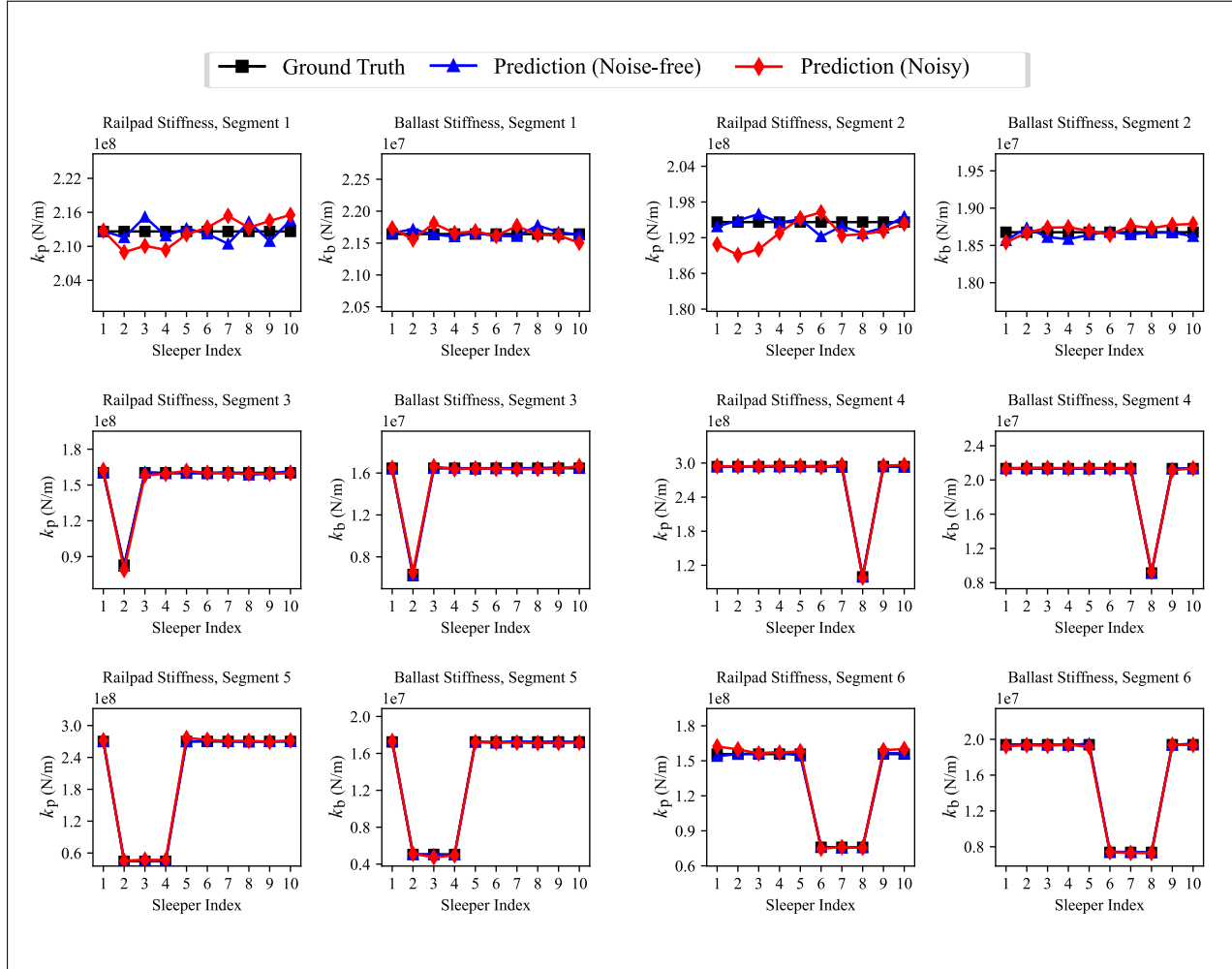


**FIGURE 5 LSTM-BiLSTM model's predictions on the noise-added test set, in the scenarios of constant and local changes of stiffness.**

investigations could explore novel feature extraction methods, including LSTM layers, for infrastructure health monitoring models.

The employed CNN and LSTM feature extractors process vibration response data in the time domain and effectively handle noisy conditions. The proposed method does not require any data preprocessing steps or handcrafted feature extraction based on expert knowledge, providing an automatic health condition monitoring algorithm capable of learning features through the training process. However, since drive-by vibration response signals are non-stationary and their components vary in both time and frequency, transformation to the frequency domain may result in a better representation of the signal. This could improve model performance but would impose further computational costs in preprocessing and may require expert knowledge in the feature extraction phase (30). Hence, Future research could explore the trade-off between different feature extraction approaches, and enhance the proposed method with the right feature extraction approach.

The proposed method effectively identifies and localizes multiple defects within the track segment, with floating locations. It simultaneously estimates railpad and ballast stiffness parameters and localizes stiffness reduction at a sleeper resolution. This enhances infrastructure monitoring tasks by providing detailed information on the type and severity of defects within the railway network. As a result, it can advance

maintenance decision-making frameworks by offering comprehensive insights into the health conditions of the systems.

The illustrative case study considers a railway track infrastructure comprising beams and beam nodes. In this context, the rails and the sleepers function as the beams of the structure, while the locations of the sleepers are considered beam nodes that transfer the load to the ballast substructure. The proposed approach involves segmenting the vibration signal into bearing spans corresponding to individual sleepers or beam nodes. This methodology shows potential for application to other infrastructures with a similar configuration of beams and beam nodes, such as bridges. Furthermore, the dataset used in this paper is based on the vehicle-track interaction finite element simulation (7), enhanced by incorporating floating defect locations and additive white Gaussian noise. Therefore, future research could explore the performance of our proposed LSTM-BiLSTM network in other case studies of infrastructure health monitoring using drive-by vibration response measurements.

## 5 CONCLUSIONS AND FUTURE WORK

In this paper, we proposed a novel method for estimating and localizing multiple physical parameters of infrastructures using drive-by vibration responses, achieved through the development of an LSTM-BiLSTM network. Our methodology emphasizes the importance of considering both forward and backward temporal information through BiLSTM networks to enhance algorithms for monitoring infrastructure health conditions. The findings demonstrate that employing BiLSTM in the higher-level health condition estimation phase can significantly reduce MAPE and RMSE, even in the presence of noise. Moreover, the methodology highlights the potential of LSTM networks for extracting features from drive-by vibration signals. By accurately identifying the positions of vibration signals, our proposed framing approach improves the resolution of infrastructure monitoring to the beam level. Hence, the LSTM-BiLSTM model effectively estimates physical parameters at various components within the infrastructure beam levels, offering comprehensive insights into the health conditions of the systems and enhancing maintenance decision-making frameworks. In the case study analyzed, the results show that the method is effective in estimating the stiffness parameters of railpads and ballast, as well as in identifying reductions in track stiffness at the level of individual sleepers. The proposed BiLSTM networks significantly decrease the Mean Absolute Percentage Error (MAPE) and Root Mean Square Error (RMSE) by nearly 50%, achieving a MAPE of 1.7% for railpad stiffness and 0.7% for ballast stiffness, even in noisy environments.

Future research will focus on assessing the proposed model's performance with other benchmarks in the literature to provide more robust conclusions on the proposed BiLSTM networks. Moreover, the feature extraction phase requires further exploration of advanced CNN and LSTM networks, alongside other preprocessing techniques for vibration response signals. The proposed framing approach requires high-accuracy signal localization, which can be challenging under certain operational conditions. In this regard, leveraging domain knowledge concerning the number and location of beam nodes in the infrastructure holds promise for addressing the location approximation challenge.

## AUTHOR CONTRIBUTIONS

The authors confirm contribution to the paper as follows: study conception and design: R.R. Samani, A. Núñez, B. De Schutter; data collection: R.R. Samani, A. Alfredo Núñez; analysis and interpretation of results: R.R. Samani, A. Núñez; draft manuscript preparation: R.R. Samani, A. Núñez, B. De Schutter. All authors reviewed the results and approved the final version of the manuscript.

## **DECLARATION OF CONFLICTING INTERESTS**

The authors declared no potential conflicts of interest with respect to the research, authorship, and/or publication of this article.

## **ACKNOWLEDGMENTS**

The first author would like to extend their gratitude to Chen Shen for providing the simulator used in this article. The first author would like to extend their gratitude to Yuanchen Zeng and Hesam Araghi for their valuable comments during the preparation of this article. This research was partly supported by ProRail and Europe's Rail Flagship Project IAM4RAIL - Holistic and Integrated Asset Management for Europe's Rail System [grant agreement 101101966].

## **DISCLAIMER**

Funded by the European Union. Views and opinion expressed are however those of the authors only and do not necessarily reflect those of the European Union. Neither the European Union nor the granting authority can be held responsible for them. This project has received funding from the European Union's Horizon Europe research and innovation programme under Grant Agreement No 101101966.

## REFERENCES

- [1] Ghofrani, F., Q. He, R. Mohammadi, A. Pathak, and A. Aref, Bayesian Survival Approach to Analyzing the Risk of Recurrent Rail Defects. *Transportation Research Record: Journal of the Transportation Research Board*, vol. 2673, 2019, pp. 281–293.
- [2] Mohammadi, R., Q. He, F. Ghofrani, A. Pathak, and A. Aref, Exploring the Relationship between Foot-by-Foot Track Geometry and Rail Defects: A Data-Driven Approach. *Presented at 98th Annual Meeting of Transportation Research Board, Washington, D.C.*, 2019.
- [3] Radzieński, M., M. Krawczuk, and M. Palacz, Improvement of Damage Detection Methods Based on Experimental Modal Parameters. *Mechanical Systems and Signal Processing*, vol. 25, 2011, pp. 2169–2190.
- [4] Neuhold, J., M. Landgraf, S. Marschnig, and P. Veit, Measurement Data-Driven Life-Cycle Management of Railway Track. *Transportation Research Record*, vol. 2674, 2020, pp. 685–696.
- [5] Nielsen, J. C., E. G. Berggren, A. Hammar, F. Jansson, and R. Bolmsvik, Degradation of Railway Track Geometry – Correlation between Track Stiffness Gradient and Differential Settlement. *Proceedings of the Institution of Mechanical Engineers, Part F: Journal of Rail and Rapid Transit*, vol. 234, 2020, pp. 108–119.
- [6] Hoelzl, C., V. Dertimanis, L. Ancu, A. Kollros, and E. Chatzi, Vold–Kalman Filter Order Tracking of Axle Box Accelerations for Track Stiffness Assessment. *Mechanical Systems and Signal Processing*, vol. 204, 2023, p. 110817.
- [7] Shen, C., P. Zhang, R. Dollevoet, A. Zoeteman, and Z. Li, Evaluating Railway Track Stiffness Using Axle Box Accelerations: A Digital Twin Approach. *Mechanical Systems and Signal Processing*, vol. 204, 2023, p. 110730.
- [8] Fernández-Bobadilla, H. A., and U. Martin, Modern Tendencies in Vehicle-Based Condition Monitoring of the Railway Track. *IEEE Transactions on Instrumentation and Measurement*, vol. 72, 2023, pp. 1–44.
- [9] Alvandi, A., and C. Cremona, Assessment of vibration-based damage identification techniques. *Journal of Sound and Vibration*, vol. 292, 2006, pp. 179–202.
- [10] Quirke, P., D. Cantero, E. J. O'Brien, and C. Bowe, Drive-by Detection of Railway Track Stiffness Variation Using in-Service Vehicles. *Proceedings of the Institution of Mechanical Engineers, Part F: Journal of Rail and Rapid Transit*, vol. 231, 2017, pp. 498–514.
- [11] Zhu, X. Q., S. S. Law, and L. Huang, Identification of Railway Ballasted Track Systems from Dynamic Responses of In-Service Trains. *Journal of Aerospace Engineering*, vol. 31, 2018, p. 04018060.
- [12] Avci, O., O. Abdeljaber, S. Kiranyaz, M. Hussein, M. Gabbouj, and D. J. Inman, A Review of Vibration-Based Damage Detection in Civil Structures: From Traditional Methods to Machine Learning and Deep Learning Applications. *Mechanical Systems and Signal Processing*, vol. 147, 2021, p. 107077.
- [13] Phusakulkajorn, W., A. Núñez, H. Wang, A. Jamshidi, A. Zoeteman, B. Ripke, R. Dollevoet, B. De Schutter, and Z. Li, Artificial Intelligence in Railway Infrastructure: Current Research, Challenges, and Future Opportunities. *Intelligent Transportation Infrastructure*, vol. 2, 2023, p. liad016.

- [14] Zaman, A., X. Liu, and Z. Zhang, Video Analytics for Railroad Safety Research: An Artificial Intelligence Approach. *Transportation Research Record*, vol. 2672, 2018, pp. 269–277.
- [15] Rafe, A., and P. A. Singleton, Imputing Time Series Pedestrian Volume Data With Consideration of Epidemiological-Environmental Variables. *Transportation Research Record*, 2024-04-18, p. 03611981241240758.
- [16] Rafe, A., and P. A. Singleton, Exploring Factors Affecting Pedestrian Crash Severity Using TabNet: A Deep Learning Approach. *Data Science for Transportation*, vol. 6, 2024, p. 13.
- [17] Yan, T.-H., M. D. A. Costa, and F. Corman, Developing and Extending Status Prediction Models for Railway Tracks Based on On-Board Monitoring Data. *Transportation Research Record*, vol. 2677, 2023, pp. 708–719.
- [18] Chellaswamy, C., T. S. Geetha, M. Surya Bhupal Rao, and A. Vanathi, Optimized Railway Track Condition Monitoring and Derailment Prevention System Supported by Cloud Technology. *Transportation Research Record*, vol. 2675, 2021, pp. 346–361.
- [19] Hajializadeh, D., Deep Learning-Based Indirect Bridge Damage Identification System. *Structural Health Monitoring*, vol. 22, 2023, pp. 897–912.
- [20] Pathirage, C. S. N., J. Li, L. Li, H. Hao, W. Liu, and P. Ni, Structural Damage Identification Based on Autoencoder Neural Networks and Deep Learning. *Engineering Structures*, vol. 172, 2018, pp. 13–28.
- [21] Huang, J., X. Yin, and S. Kaewunruen, Quantification of Dynamic Track Stiffness Using Machine Learning. *IEEE Access*, vol. 10, 2022, pp. 78747–78753.
- [22] Le-Xuan, T., T. Bui-Tien, and H. Tran-Ngoc, A Novel Approach Model Design for Signal Data Using 1DCNN Combing with LSTM and ResNet for Damaged Detection Problem. *Structures*, vol. 59, 2024, p. 105784.
- [23] Jie, L., L. Fang, X. Weiping, and J. Xiaoxiong, Track Vibration Sequence Anomaly Detection Algorithm Based on LSTM. *Advances in Structural Engineering*, vol. 26, 2023, pp. 1682–1695.
- [24] Sharma, S., and S. Sen, Real-Time Structural Damage Assessment Using LSTM Networks: Regression and Classification Approaches. *Neural Computing and Applications*, vol. 35, 2023, pp. 557–572.
- [25] Hochreiter, S., and J. Schmidhuber, Long Short-Term Memory. *Neural Computation*, vol. 9, 1997, pp. 1735–1780.
- [26] Shen, C., R. Dollevoet, and Z. Li, Fast and Robust Identification of Railway Track Stiffness from Simple Field Measurement. *Mechanical Systems and Signal Processing*, vol. 152, 2021, p. 107431.
- [27] Lamprea-Pineda, A. C., D. P. Connolly, A. Castanheira-Pinto, P. Alves-Costa, M. F. Hussein, and P. K. Woodward, On Railway Track Receptance. *Soil Dynamics and Earthquake Engineering*, vol. 177, 2024, p. 108331.
- [28] Malhotra, P., A. Ramakrishnan, G. Anand, L. Vig, P. Agarwal, and G. Shroff, LSTM-based Encoder-Decoder for Multi-sensor Anomaly Detection. *ICML 2016 Anomaly Detection Workshop*, New York, NY, 2016, URL <https://doi.org/10.48550/arXiv.1607.00148>.
- [29] Hou, B., J. Yang, P. Wang, and R. Yan, LSTM-Based Auto-Encoder Model for ECG Arrhythmias Classification. *IEEE Transactions on Instrumentation and Measurement*, vol. 69, 2020, pp. 1232–1240.

[30] Nossier, S. A., J. Wall, M. Moniri, C. Glackin, and N. Cannings, A Comparative Study of Time and Frequency Domain Approaches to Deep Learning Based Speech Enhancement. In *2020 International Joint Conference on Neural Networks (IJCNN)*, 2020, pp. 1–8.